Environment International 118 (2018) 48–59

Contents lists available at ScienceDirect

Environment International

journal homepage: www.elsevier.com/locate/envint

Short-term effects of airport-associated ultrafine particle exposure on lung function and inflammation in adults with asthma

Rima Habre[a,*], Hui Zhou[a], Sandrah P. Eckel[b], Temuulen Enebish[a], Scott Fruin[a], Theresa Bastain[a], Edward Rappaport[a], Frank Gilliland[a]

[a] Division of Environmental Health, Department of Preventive Medicine, Keck School of Medicine, University of Southern California, Los Angeles, CA, USA
[b] Division of Biostatistics, Department of Preventive Medicine, Keck School of Medicine, University of Southern California, Los Angeles, CA, USA

ARTICLE INFO

Editor: Xavier Querol

ABSTRACT

Background: Exposure to ultrafine particles (UFP, particles with aerodynamic diameter < 100 nm) is associated with reduced lung function and airway inflammation in individuals with asthma. Recently, elevated UFP number concentrations (PN) from aircraft landing and takeoff activity were identified downwind of the Los Angeles International Airport (LAX) but little is known about the health impacts of airport-related UFP exposure.

Methods: We conducted a randomized crossover study of 22 non-smoking adults with mild to moderate asthma in Nov-Dec 2014 and May-Jul 2015 to investigate short-term effects of exposure to LAX airport-related UFPs. Participants conducted scripted, mild walking activity on two occasions in public parks inside (exposure) and outside (control) of the high UFP zone. Spirometry, multiple flow exhaled nitric oxide, and circulating inflammatory cytokines were measured before and after exposure. Personal UFP PN and lung deposited surface area (LDSA) and stationary UFP PN, black carbon (BC), particle-bound PAHs (PB-PAH), ozone (O_3), carbon dioxide (CO_2) and particulate matter ($PM_{2.5}$) mass were measured. Source apportionment analysis was conducted to distinguish aircraft from roadway traffic related UFP sources. Health models investigated within-subject changes in outcomes as a function of pollutants and source factors.

Results: A high two-hour walking period average contrast of ~34,000 particles·cm^{-3} was achieved with mean (std) PN concentrations of 53,342 (25,529) and 19,557 (11,131) particles·cm^{-3} and mean (std) particle size of 28.7 (9.5) and 33.2 (11.5) at the exposure and control site, respectively. Principal components analysis differentiated airport UFPs (PN), roadway traffic (BC, PB-PAH), PM mass ($PM_{2.5}$, PM_{10}), and secondary photochemistry (O_3) sources. A standard deviation increase in the 'Airport UFPs' factor was significantly associated with IL-6, a circulating marker of inflammation (single-pollutant model: 0.21, 95% CI = 0.08–0.34; multi-pollutant model: 0.18, 0.04–0.32). The 'Traffic' factor was significantly associated with lower Forced Expiratory Volume in 1 s (FEV_1) (single-pollutant model: −1.52, −2.28 to −0.77) and elevated sTNFrII (single-pollutant model: 36.47; 6.03–66.91; multi-pollutant model: 64.38; 6.30–122.46). No consistent associations were observed with exhaled nitric oxide.

Conclusions: To our knowledge, our study is the first to demonstrate increased acute systemic inflammation following exposure to airport-related UFPs. Health effects associated with roadway traffic exposure were distinct. This study emphasizes the importance of multi-pollutant measurements and modeling techniques to disentangle sources of UFPs contributing to the complex urban air pollution mixture and to evaluate population health risks.

1. Introduction

Exposure to ultrafine particles (UFP, particles with aerodynamic diameter < 100 nm) in ambient air is associated with decreased lung function and increased airway inflammation in individuals with asthma (Buonanno et al., 2013; Heinzerling et al., 2016; McCreanor et al., 2007). While fresh fuel combustion and roadway traffic sources have long been recognized as major primary sources of UFPs (Hofman et al., 2016; Kukkonen et al., 2016), only recently have measurement campaigns shown aircraft traffic activity to be a significant source of UFPs, with elevated particle number (PN) concentrations in close proximity to runways (Hsu et al., 2012; Hsu et al., 2013; Westerdahl et al., 2008) and

* Corresponding author at: Division of Environmental Health, USC Keck School of Medicine, 2001 N Soto St, Rm 102M, Los Angeles, CA 90089, USA.
E-mail address: habre@usc.edu (R. Habre).

https://doi.org/10.1016/j.envint.2018.05.031
Received 20 January 2018; Received in revised form 30 April 2018; Accepted 15 May 2018
Available online 26 May 2018

further downwind of airports (ACI Europe, 2012; Choi et al., 2013; Hsu et al., 2014; Hudda et al., 2014; Hudda and Fruin, 2016; Hudda et al., 2016; Keuken et al., 2015). In Los Angeles, CA, Hudda et al. (2014) showed that PN concentrations downwind of the Los Angeles International Airport (LAX) are at least twice as high as background during most hours of the day with a 4- to 5-fold increase up to 10 km under typical westerly wind conditions.

Inflammation and oxidative stress are thought to be the main pathways of UFP toxicity. Because of their smaller size and diffusion-driven behavior in the lungs once inhaled, UFPs deposit efficiently in the alveolar region (Delfino et al., 2005). Once there, they can evade macrophage clearance, enter lung cells, cross the epithelial barrier into the blood and lymphatic circulation, elicit systemic effects and reach other organs (Elder et al., 2006; Geiser, 2010; Nemmar et al., 2004; Samet et al., 2009). They can also damage airway epithelial cells and macrophages via reactive oxygen species production from redox reactions occurring in the mitochondria (Li et al., 2003; Nel, 2005). UFPs are also retained very effectively in the lungs and can remain there for long periods of time (Araujo and Nel, 2009). Surface coating is important in determining mucus penetration potential and retention time in the lungs, where biodegradable, hydrophilic or negatively charged UFPs can evade adhesive interactions with the mucus mesh or diffuse through pores, reach the adherent mucus layer and evade rapid clearance (Lai et al., 2009; Schuster et al., 2013; Xu et al., 2013). Möller et al. (2008) showed that most inhaled carbon UFPs are retained in the lung periphery and conducting airways without substantial systemic translocation 48 h after exposure. In addition, their large surface area to mass ratio and ability to carry reactive oxygen generating species such as metals (Vitkina et al., 2016) and PAHs (Delfino et al., 2010) on their surface (redox potential) makes them more toxic than larger particles such as $PM_{2.5}$ (particles with aerodynamic diameter $< 2.5\,\mu m$) on an equal mass basis (Ayres et al., 2008; Cho et al., 2005; Gong et al., 2014; Nel et al., 2001; Sioutas et al., 2005). Weichenthal et al. (2007) provide an excellent review of in vitro, in vivo and population studies of UFPs, their composition and mode of action.

Epidemiological evidence of UFP health effects is limited compared to $PM_{2.5}$, likely due to their highly dynamic and variable nature in space and time which complicates exposure assessment (2013). Wichmann et al. (2000) provide a review of the epidemiological evidence on short-term health effects of UFPs and explain the potentially independent physiological pathways by which UFPs induce toxicity compared to $PM_{2.5}$ also demonstrated in Gong et al. (2014) Generally longer exposure-response lag times are observed in panel studies for UFPs, possibly related to their longer retention time in the lungs. Buonanno et al. (2013) found daily UFP alveolar-deposited surface area dose to be associated with exhaled nitric oxide, a marker of pulmonary inflammation, in asthmatic children. Delfino et al. (2009) found "quasi-UFPs" (particles with aerodynamic diameter $< 0.25\,\mu m$) to be significantly associated with the inflammation markers IL-6 and soluble TNF-α. Roadway traffic studies also suggest that fresh combustion products in exhaust - of which UFP is a large component - play a major role in asthma attacks and chronic bronchitis (Brauer et al., 2002; Kunzli et al., 2000), cause acute decreases in lung function that is more pronounced in asthmatics (McCreanor et al., 2007), and may be a cause of asthma (Brauer et al., 2002; Gauderman et al., 2005; McConnell et al., 2006). Knibbs et al. (2011) reviewed 10 studies of commuter exposure in-transit and found UFP exposure during commuting can elicit acute effects in both healthy and health-compromised individuals. Lanzinger et al. (2016) found 0–5 day lag central site UFP levels were associated with respiratory mortality independent of particle mass in five central European cities.

Cardiovascular effects have also been reported especially in individuals with existing metabolic or cardiovascular conditions. Lag 4-day PN was associated with total and cardio-respiratory mortality in Germany (Stolzel et al., 2007). Thrombogenic effects and platelet activation were seen in patients with coronary heart disease (Ruckerl et al., 2006). An increase in pulse wave velocity and augmentation index was seen in individuals with chronic obstructive pulmonary disease (Sinharay et al., 2018) and immediate changes in heart rate variability were found in diabetics or people with impaired glucose metabolism (Peters et al., 2015).

However, very few studies have investigated the effects of UFPs resulting from aviation activity on asthma and respiratory health. Children living in 17 Massachusetts communities within a 5-mile radius of the Boston Logan International Airport were 3 to 4 times more likely to experience respiratory symptoms indicative of undiagnosed asthma compared to low exposure areas (Massachusetts Department of Public Health, 2014). Schlenker and Walker (2011) estimated that one standard deviation increase in daily air pollution levels attributable to runway congestion at the 12 largest airports in California leads to an additional $1 million in hospitalization costs for respiratory and heart related admissions, for the 6 million individuals living within 10 km. However, these studies relied on spatially coarse estimates of residential exposure that suffer from exposure measurement error in estimating personal exposures.

To our knowledge, no studies to date have assessed personal exposure to real-life, airport-related UFPs, distinctly from roadway traffic-related UFPs, and investigated their effect on acute respiratory health in asthmatics. To this end, we conducted a quasi-experimental panel study designed to capture the high UFP plume downwind of LAX reported in Hudda et al. (2014). We hypothesized that short-term exposure to LAX-related UFPs results in acute decreased pulmonary function and increased pulmonary and systemic inflammation in adult asthmatics following mild walking activity.

2. Methods

2.1. Study design

We conducted a randomized crossover study of 22 adults in two phases, Nov–Dec 2014 and May–July 2015, modeled after the McCreanor et al. (2007) quasi-experimental design. Eligibility criteria included the following: Non-current smokers (zero cigarettes smoked in the last month, regardless of earlier smoking history), English-speaking (individuals who can speak and understand English for the sake of communicating with study staff and answering questions, since it was not feasible to translate study materials into other languages), and adults aged 18 years or older with mild to moderate asthma as defined by symptoms-based National Heart, Lung and Blood Institute (NHLBI) criteria. Participants were mainly recruited as a convenience sample by advertising to University of Southern California (USC) staff and students.

Participants conducted mild, scripted walking activity for 2 h, resting every 15 min, on two occasions in two public parks inside and outside of the high LAX UFP zone reported in Hudda et al. (2014). We selected Jesse Owens Park as the 'exposure' site because of its location downwind of LAX, ~10 km to the east along the dominant daytime westerly wind direction (supplement Fig. S1). Jesse Owens is in a dense urban area near busy, major roadways (W Century Blvd to the south and S Western Ave to the east). We selected Kenneth Hahn State Recreational Area as the 'control' site, ~9 km northeast of LAX, as it is located on a hill at the periphery of the high UFP plume, surrounded by greenness and further away from immediate traffic. The order of the visits to the control and exposure sites was randomized, and the visits were separated by at least one week to minimize carryover effects.

We transported participants to and from the walking sites in a 2015 Toyota Prius hybrid car, under recirculating air and closed window conditions, along pre-designated routes to minimize UFP exposure from traffic. To ensure maximum LAX UFP impacts, we visited the exposure site on days with stable midday westerly wind conditions, to the extent logistically possible. We conducted all walking exposures midday (~12–2 PM) to control for diurnal variations and ensure maximum

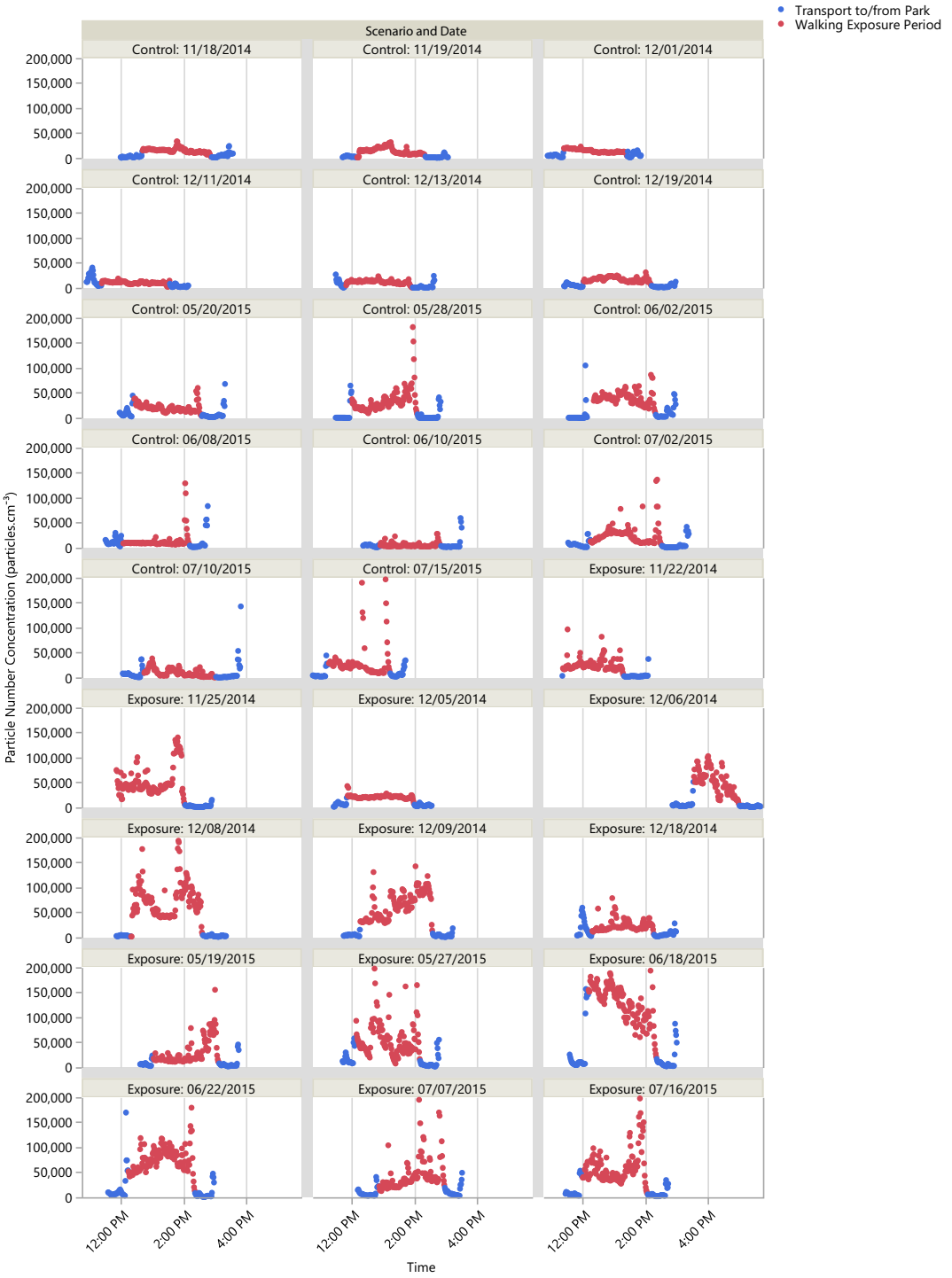

Fig. 1. Ultrafine particle number concentrations (PN, particles·cm^{-3}) on study days grouped by exposure scenario and colored by transport (blue) and walking exposure (red) period. (For interpretation of the references to color in this figure legend, the reader is referred to the web version of this article.)

wind direction stability. The USC Institutional Review Board approved all study procedures (IRB protocol number HS-14-00504), and all participants provided written informed consent and were compensated for their contribution to the study.

2.2. Health outcomes assessment

Participants reported to the USC Health Sciences Campus in the morning on both study days. In the first visit, we collected detailed demographics, medical history, environmental conditions at the residence, and commuting and time activity patterns using an interviewer-administered questionnaire. We measured height (stadiometer), weight and body composition (Tanita scale) and resting heart rate at baseline. In addition, on each visit, we administered a questionnaire asking about the prior week's activities, asthma control and severity, as well as their morning commute and dietary intake on the day of the visit.

Respiratory testing and blood draws were performed on each visit before and after exposure at generally similar, consistent times visit-to-visit for each person and across participants (~10.30 AM and 4.00 PM).

We conducted multiple flow exhaled nitric oxide testing (FeNO) using our previously developed protocol at 30, 50, 100 and 300 ml/s expiratory flow rates using the EcoMedics CLD88-SP with DeNOx (Linn et al., 2009). Immediately prior to each maneuver, the participant breathed through a DeNOx scrubber for ≥2 tidal breaths followed by inhalation to total lung capacity and exhalation at the target flow rate. Analyzer zero checks against air drawn through a zero-NO filter (Sievers Division, GE Analytical Instruments, Boulder, CO) were done twice daily. A Morgan SpiroAir-LT rolling seal spirometer was used for pulmonary function testing (forced vital capacity (FVC), forced expiratory volume in 1 s (FEV_1), peak expiratory flow rate (PEFR), and maximum mid-expiratory flow (MMEF)) and calibrated twice daily with a 3 l syringe and tested for leaks. Each participant was asked to perform seven maximum effort maneuvers per test.

An Immunocap antigen-specific IgE panel (Quest Diagnostics, Inc.) for the 16 most common Southern California upper respiratory allergens was conducted using the first blood sample to determine atopic status at baseline. A complete blood count was also obtained using the morning blood draw on each visit. In addition, pre- and post-exposure blood samples on both visits were analyzed for the following inflammatory cytokines and pro-thrombotic clotting factors: high-sensitivity Interleukin 6 (IL-6) and soluble tumor necrosis factor receptor II (sTNFrII) using ELISA kits (R&D Systems, HS600B and DRT200 respectively), and von Willebran factor (vWF) and fibrinogen using the Millipore Luminex magnetic bead panel (HCVD3MAG-67 K).

2.3. Air pollution exposure assessment

During transport to and from the parks, we measured ultrafine particle number (PN) concentrations using a DiscMini diffusion charger (Testo AG) and condensation particle counter (CPC 3007, TSI Inc.) to verify low traffic-related UFP exposure conditions inside the vehicle. During the walking exposure period at the parks, we measured 'personal' PN, particle size and lung deposited surface area (LDSA) using the DiscMini and PN using the CPC carried by the research assistant walking alongside the participants. Relative humidity and temperature were measured using an Onset HOBO data logger. We also used a mobile monitoring platform to measure PN (CPC 3007, TSI Inc.), black carbon (BC, AE51, Magee Scientific), particle-bound PAHs (PB-PAH, PAS 2000, EchoChem Analytics), ozone (O_3, Model 205, 2B Technologies), carbon dioxide (CO_2, Li-820, LI-COR Biosciences) and particulate matter mass in four size fractions (PM_1, $PM_{2.5}$, PM_4 and PM_{10}, DRX 8534, TSI Inc.) at each park in a stationary location to obtain more detailed characterization of the air pollution mixture. All exposures were continuously logged at a 10 s time resolution. The DiscMini was considered the primary source of personal PN exposure data as it also provided particle size and LDSA data. Unless otherwise stated, all subsequent references to PN correspond to DiscMini data. Agreement between the personal DiscMini and CPC measurements in terms of PN by particle size bins are shown in the Fig. S2.

2.4. Statistical analysis

2.4.1. Air pollution exposures

We inspected all air pollutant measurement data for outliers and errors at the original 10 s time resolution and averaged up to 1 min for use in source apportionment analyses (described below). We then calculated average concentration for the transport periods to and from the park (inside the vehicle) and the walking period at the parks (exposure time) for use in health models.

Because of the highly correlated multi-pollutant nature of the data, we conducted a source apportionment analysis on the one-minute, walking-period data (shown in red in Fig. 1) to disentangle the impact of the airport from other major sources of UFPs contributing to the complex air pollution mixture in this urban area (mainly traffic). We used principal components analysis (PCA) with an oblique (promax) rotation in SAS 9.4 (SAS Institute Inc., NC). Ten variables were included in the PCA (PM_1, $PM_{2.5}$, PM_{10}, BC, PB-PAH, CO_2, PN (personal DiscMini), PN (stationary CPC), particle size, and O_3). Four distinct 'source factors' were resolved based on their eigenvalues (profiles), physical interpretability and least factor smearing. Walking-period average PCA-derived factor scores (eigenvectors) were then calculated for each day and used as the main exposures of interest in the health models, in addition to the measured pollutants.

2.4.2. Spirometry and exhaled nitric oxide

Pulmonary function test indices (FVC, FEV_1, PEFR, MMEF) were assigned based on criteria described in the 2005 ATS/ERS (Miller et al., 2005). Age, height, gender and race specific percent predicted values were calculated based on equations from Knudson et al. (1983).

FeNO data processing was based on the ATS/ERS guidelines for FeNO at 50 ml/s (ATS/ERS, 2005) and an airway turnover search window (Puckett et al., 2010) similar to previous studies (Eckel et al., 2016). $FeNO_{50}$ and $FeNO_{300}$ were calculated as the average of reproducible maneuvers at 50 ml/s and 300 ml/s, respectively. Multiple flow FeNO data were input to nonlinear mixed effects models (based on the deterministic, steady-state two compartment model of NO in the lower respiratory tract) to estimate parameters quantifying airway ($D_{aw}NO$ – airway wall tissue diffusing capacity ($pl(s{\cdot}ppb)^{-1}$), $C_{aw}NO$ – airway wall concentration (ppb)) and alveolar (C_ANO –alveolar region concentration (ppb)) sources of NO and to predict $FeNO_{50}$ (Eckel and Salam, 2013; Eckel et al., 2014). We used predicted $FeNO_{50}$ rather than measured $FeNO_{50}$ in health models to minimize the number of missing observations.

2.4.3. Health models

Single-, two- and multi-pollutant ANCOVA (Analysis of Covariance) models examining within-subject changes in outcome related to the exposures were fit as follows:

$$Y_{ij,POST} = \beta_0 + \beta_1 * Y_{ij,PRE} + \beta_2 * \text{Exposure(s)}_{ij} + U_i + \varepsilon_{ij}; \quad (1)$$

where $Y_{ij,POST}$ is the outcome measured post-exposure for participant i on day j, $Y_{ij,PRE}$ is the outcome measured pre-exposure, Exposure(s)_{ij} is one or more continuous measure(s) of the walking-period average air pollution concentration or source factor contribution on day j, U_i is a fixed intercept for every participant, and ε_{ij} is a normally distributed random error term with variance σ^2 ($\varepsilon_{ij} \sim N(0,\sigma^2)$). β_0 is a fixed intercept, β_1 is the parameter estimate capturing visit-to-visit variability in the baseline outcome, and β_2 is the main parameter of interest capturing the effect of air pollution exposure(s) (Metcalfe, 2010).

Outcomes were examined for normality and log-transformed where appropriate (FeNO parameters). Multi-pollutant models of measured concentrations were adjusted for PN, BC, $PM_{2.5}$ and O_3 – the key source tracers identified in the source apportionment modeling. Whereas multi-pollutant models of sources were adjusted for all four modeled source factors. All reported effect sizes are scaled to a standard deviation (SD) increase in the exposure of interest.

Outliers were examined and excluded as appropriate for the different sets of health outcomes (1 to 3 data points depending on outcome). The model focuses on within-participant changes in health outcomes and includes an intercept for each participant, thus there is no need to adjust for time-constant individual-level covariates such as age or gender. Given the limited sample size, a list of binary variables was selected a priori based on the literature, with at least 40% of participants in a cell, to investigate interactions with the main exposures of interest (PN, LDSA and Airport UFPs factor) in single- and multi-pollutant models: asthma control, allergic status (reported or measured using specific IgE panel), race and ethnicity, physical activity levels, body mass and composition and commuting patterns (further details in Table S1). Models with significant interaction terms were reported. For all hypothesis tests, the threshold of statistical significance was defined as p-value < 0.05; analyses were conducted in SAS 9.3 (SAS Institute Inc., Cary, NC, USA).

Table 1
Participant characteristics ($N = 22$).

		N (%)
Gender	Female	16 (73%)
Race	White	11 (50%)
	African-American	3 (14%)
	Asian	3 (14%)
	American Indian	1 (5%)
	Other	4 (18%)
Ethnicity	Hispanic	9 (43%)

	Mean	Std Dev	Min	Max
Age	27	9.5	18	60
Age at asthma diagnosis	13	12.7	3	58
ACT[a] Score (At recruitment)	18.7	3.2	11	22
ACT[a] Score (On day of visit)	20.6	3.8	11	25
Body Mass Index (kg/m^2)	24.8	6.1	17.4	46.7

[a] ACT = Asthma Control Test.

3. Results

The majority of the 22 participants in the study were female (16, 73%), white (9, 43%) and Hispanic (9, 43%). The mean age was 27 years (range 18–60) and mean BMI 24.8 kg/m^2 (17.4–46.7). The average Asthma Control Test (ACT) score was 18.7 (11 − 22) at recruitment and 20.6 (11–25) on the day of the first visit. All participants reported a doctor diagnosis of asthma at mean age of 13 years (3–58) (Table 1).

The top 5 most common upper airway allergens as measured with a specific IgE response were dust mites (d1 and d2), followed by dog (e5) and cat (e1) dander and Bermuda grass (g2), respectively. Baseline levels of cytokines, spirometry and FeNO parameters are shown in Table 2 with average change in post-exposure value compared to pre-exposure at each of the sites. Predicted $FeNO_{50}$ was highly correlated with measured $FeNO_{50}$ ($r = 0.99$).

Table 3 shows the distribution of air pollutant concentrations during the walking period at the two sites. UFP PN (stationary and personal) was significantly higher at the exposure site per study design, with an average two-hour walking period PN contrast of ~ 34,000 particles·cm^{-3} between the two sites. Fig. 1 shows the time-resolved personal PN (DiscMini) measurements for each study day grouped by site. Fig. S3 shows the distribution of PN and LDSA inside the vehicle during participant transport to and from the exposure sites. Particle size was lower at the exposure site (28.7 vs 33.2 nm) and LDSA was higher (64.8 vs 28.8 cm^2) consistent with the smaller particle size and greater lung deposition efficiency of airport-related UFPs. Particle mass concentrations in the 1, 2.5, 4 and 10 µm size fractions were slightly but not significantly higher, while the combustion-related pollutants BC, CO_2 and PB-PAHs were significantly higher at the exposure site. No differences in O_3 concentration or meteorological parameters were observed (Table 3). The second phase of the study (May–July 2015) was characterized by breezier conditions and warmer temperatures compared to the first phase (Nov–Dec 2014) and generally more stable and predictable wind direction patterns (Fig. S4).

The source apportionment analysis resolved four distinct source factors characterized by the following species in their loading profiles in parentheses: Airport UFPs (personal and stationary PN, smallest particle size) consistent with jet emissions (Shirmohammadi et al., 2017), PM Mass (PM_1, $PM_{2.5}$ and PM_{10} mass) consistent with heavier particles and wind-blown dust, Traffic (BC, CO_2, PB-PAH and lowest O_3) consistent with fresh combustion emissions and O_3 quenching, and secondary photochemistry ($PM_{2.5}$ mass and O_3) consistent with secondary formation (Table 4). The contributions of these modeled source factors were all significantly higher at the exposure site except for 'PM Mass' (Table 3). The 'Secondary Photochemistry' and 'PM Mass' factors were most highly correlated (Table S2). The average contributions of the 'Airport UFPs' and 'Secondary Photochemistry' factors were higher in the second phase while 'Traffic' was higher in the first phase of the study likely due to cooler temperatures and less vertical mixing (Fig. S5).

Single- and multi-pollutant health analysis results are reported in Tables 5 and 6, respectively, while two-pollutant results are included in Supplement Table S3. Adjustment for day-level, time-varying potential confounders such as relative humidity and temperature was explored but did not have any influence on the magnitude of main effects in PN and 'Airport UFPs' models.

The strongest evidence for associations were for the 'Airport UFPs' source with IL-6, $PM_{2.5}$ and 'Traffic' with FEV_1, and 'Traffic' with sTNFrII. The 'Airport UFPs' source – characterized by high PN and low particle size, our main hypothesized exposure of interest - was significantly associated with IL-6 in all models (0.18, 0.04–0.32 in multi-pollutant model) and was robust to all adjustments. The correlation

Table 2
Distribution of health outcomes at baseline (morning assessment on first visit) and change (post-pre) in outcomes following walking exposure period at the two study sites.

Outcome	Baseline level					Change (Post-Pre)						
						Control			Exposure			
	N	Mean	Std Dev	Min	Median	Max	N	Mean	Std Dev	N	Mean	Std Dev
Cytokines (pg/ml)												
IL-6	18	1.7	2.8	0.4	0.8	12.3	20	0.3	1.7	18	0.4	0.4
sTNFrII	18	1083.1	922.9	146.2	940.6	2384.0	20	−79.0	131.7	18	−85.6	87.8
vWF	17	0.5	0.2	0.3	0.5	0.8	18	0.0	0.2	18	0.0	0.1
Fibrinogen	17	78.4	29.6	45.4	67.4	127.6	18	0.6	19.7	18	−0.5	19.9
% Predicted spirometry												
FEV_1	22	105.0	14.5	72.3	105.7	132.8	21	0.0	4.2	22	−1.2	3.4
FVC	22	108.9	11.3	80.5	108.4	129.0	20	−0.8	2.8	22	−0.7	3.1
MMEF	22	99.9	30.4	34.2	96.9	153.5	20	−0.3	9.5	22	−0.7	9.2
PEFR	22	107.4	24.1	59.6	105.6	152.6	21	3.0	8.4	22	2.1	10.3
Exhaled nitric oxide[a]												
$\log(FeNO_{50,pred})$	22	3.30	0.8	2.2	3.0	4.6	21	0.0	0.1	22	−0.1	0.1
C_ANO	22	1.1	0.9	−0.7	1.2	2.5	21	0.0	0.2	22	−0.2	0.3
$\log(C_{AW}NO)$	22	4.0	0.9	2.7	3.8	5.6	21	0.0	0.2	22	−0.1	0.3
$\log(D_{AW}NO)$	22	3.6	0.6	2.4	3.5	4.8	21	0.0	0.2	22	0.1	0.3

[a] Exhaled nitric oxide units as follows: $\log(FeNO_{50})$ in log(ppb); CANO and $\log(C_{AW}NO)$ in log(ppb); $\log(D_{AW}NO)$ in log(pl(s·ppb)$^{-1}$).

Table 3
Distribution of air pollution exposure and meteorology parameters during the walking periods.

	Overall (n = 43)		Control (n = 21)		Exposure (n = 22)		Pearson t-test
	Mean	Std Dev	Mean	Std Dev	Mean	Std Dev	p-Value
Pollutants (units)							
PN (particles·cm^{-3}, personal DiscMini)	36,842.2	26,016.4	19,556.6	11,131.0	53,342.1	25,528.5	3.97E-06
Particle size (nm)	30.9	10.6	33.2	11.5	28.7	9.5	1.67E-01
LDSA (cm^2)	47.2	27.1	28.8	13.0	64.8	25.4	1.59E-06
PN (particles·cm^{-3}, stationary CPC)	23,013.6	14,062.5	13,036.0	4491.7	32,537.6	13,480.1	8.66E-07
PN (particles·cm^{-3}, personal CPC)	31,705.0	18,589.5	19,066.1	6879.7	43,769.4	18,271.3	2.60E-06
PM_1 (μg/m^3)	4.7	3.6	3.9	2.7	5.5	4.2	1.56E-01
$PM_{2.5}$ (μg/m^3)	12.0	7.6	10.1	5.8	13.7	8.8	1.17E-01
PM_4 (μg/m^3)	14.8	8.8	12.7	6.7	16.9	10.2	1.24E-01
PM_{10} (μg/m^3)	30.1	22.1	27.4	12.3	32.6	28.7	4.42E-01
BC (ng/m^3)	523.5	291.9	410.0	207.3	631.9	322.9	1.09E-02
CO_2 (ppb)	407.8	13.3	401.4	9.3	413.9	13.8	1.28E-03
PB-PAH (μg/m^3)	3.2	1.5	2.6	0.6	3.8	1.9	8.07E-03
O_3 (ppb)	45.9	14.4	44.9	12.0	46.7	16.7	6.89E-01
Source factors							
Airport UFPs	0.06	0.74	−0.32	0.49	0.42	0.77	5.91E-04
PM mass	−0.05	0.46	−0.14	0.33	0.04	0.55	1.85E-01
Traffic	−0.14	0.86	−0.53	0.58	0.23	0.92	2.45E-03
Secondary photochemistry	−0.04	0.80	−0.31	0.62	0.21	0.88	3.06E-02
Meteorology							
Temperature (°C)	27.05	2.74	26.3	2.5	27.7	2.8	9.58E-02
Relative humidity (%)	45.02	9.32	46.5	8.1	43.6	10.3	3.21E-01

PN = Ultrafine Particle Number, LDSA = Lung-deposited surface area, PM_1, $PM_{2.5}$, PM_4, PM_{10} = Particle Mass in the 1, 2.5, 4 and 10 μm size fraction, BC = Black Carbon, CO_2 = Carbon Dioxide, PB-PAH = Particle-bound Polyaromatic Hydrocarbons, O_3 = Ozone.
The overall standard deviation is used to scale reported health effect estimates.

Table 4
Loading profiles (eigenvalues) of air pollution source factors resolved by principal components analysis.

Pollutant	Source factors			
	Airport UFPs	PM Mass	Traffic	Secondary photochemistry
PN (personal DiscMini)	0.72	0.00	0.16	0.20
PN (stationary CPC)	0.71	−0.02	0.35	0.19
Particle Size	−0.81	0.01	0.23	0.15
PM_1	−0.04	0.93	0.07	0.06
$PM_{2.5}$	−0.10	0.63	0.09	0.47
PM_{10}	0.07	0.98	−0.07	−0.08
BC	0.05	0.17	0.76	−0.14
CO_2	−0.03	−0.10	0.83	−0.10
PB-PAH	0.19	0.07	0.59	−0.21
O_3	0.19	0.06	−0.63	0.68

between DiscMini and CPC PN measurements varied by particle size (Fig. S2), and health model results were slightly different by instrument (Table S5) with generally stronger IL-6 effects seen with the CPC. Contrary to what we expected, IL-6 had a stronger association with PN than LDSA. None of the other systemic or pulmonary inflammation or lung function metrics were positively associated with PN or the 'Airport UFPs' source in our study.

For lung function, measured PM (PM_1, $PM_{2.5}$, PM_4 and PM_{10}) and the modeled 'PM Mass' source were all associated with lower FEV_1 and MMEF in single-pollutant models. For example, a 1 SD increase in $PM_{2.5}$ (7.6 μg/m^3) was associated with 1.45% and 2.98% drop in % predicted FEV_1 and MMEF, respectively. Effect estimates were even larger for PM_{10} (2.02% and 5.56%, respectively). Similarly, in multi-pollutant models, $PM_{2.5}$ was associated with 1.92% and 5.31% drop in % predicted FEV_1 and MMEF, respectively. Measured $PM_{2.5}$ was more strongly associated with lower FEV_1 and MMEF compared to the modeled 'PM Mass' source in all models. FEV_1 was also negatively associated with BC (−1.60, −2.68 to −0.51) in single-pollutant models and the modeled 'Traffic' source in the single-pollutant model (−1.52, −2.28 to −0.77).

sTNFrII had consistent and significant positive associations with the modeled 'Traffic' source factor in single- and multi-pollutant models, and with measured BC and PB-PAH in single-pollutant models. In single-pollutant models, sTNFrII increased by: 36.5 pg/ml (95% CI 6.0–66.9) per SD increase in 'Traffic', 49.4 pg/ml (10.2–88.6) per SD (292 ng/m^3) increase in BC, and 30.2 pg/ml (1.6–58.9) per SD (1.5 μg/m^3) increase in PB-PAHs. In multi-pollutant models, the 'Traffic' effect increased to 64.4 pg/ml (6.3–122.5).

Less consistent associations were observed with the other measured pollutants or modeled source factors and other health outcomes. A significant negative association of $PM_{2.5}$ mass with IL-6 was found in single- and multi-pollutant models; however, the 'PM mass' source factor and IL-6 association was marginally significant (negative) in single-pollutant models but positive and non-significant in multi-pollutant models. PN exposure was associated with decreased log(C_{AW}NO) in single- and two-pollutant models; however, this association became non-significant in multi-pollutant models. Finally, O_3 exhibited results that were contrary to the expected direction in single- and two-pollutant models with FEV_1 and sTNFrII and with FEV_1 in multi-pollutant models. Similarly, 'Secondary Photochemistry' exhibited associations in the opposite direction of what is expected for IL-6 (single-pollutant model) and C_ANO (adjusted for 'Airport UFPs'); however, all associations became non-significant in multi-pollutant models.

Models with significant interaction terms ($p < 0.05$) are reported in Fig. S6 and Table S4. Given the limited sample size, multiple tests, and underpowered statistical analysis of interactions, these results should only be interpreted qualitatively. While interaction results were generally inconsistent, Hispanic ethnicity was associated with poorer % predicted PEFR following 'Airport UFPs' exposure compared to non-Hispanic ethnicity; whereas, being non-Hispanic was associated with higher log(D_{AW}NO) response following PN exposure. Finally, having high muscle mass (> median 45.1 kg) and being sick in the last month were 'protective' following 'Airport UFPs' and PN exposure, respectively.

Table 5
Single-pollutant model associations of measured concentrations and modeled source factor contributions with cytokines, exhaled nitric oxide and spirometry outcomes.

Pollutants

Outcome	N	PN			LDSA			BC			PB-PAH			O_3		
		Est	95% CI	*p*-Value	Est	95% CI	*p*-Value	Est	95% CI	*p*-Value	Est	95% CI	*p*-Value	Est	95% CI	*p*-Value
Cytokines																
IL-6	36	0.13	−0.03, 0.29	0.100	0.07	−0.11, 0.25	0.407	−0.09	−0.31, 0.12	0.373	0.05	−0.11, 0.20	0.523	0.03	−0.20, 0.27	0.751
Fibrinogen	35	−0.01	−9.83, 9.82	0.999	−0.98	−11.21, 9.25	0.841	−3.07	−14.23, 8.09	0.565	−2.99	−11.76, 5.77	0.476	4.64	−7.36, 16.64	0.421
sTNFrII	36	10.57	−24.06, 45.19	0.525	21.03	−14.18, 56.24	0.222	49.38	10.18, 88.59	0.017	30.23	1.55, 58.92	0.040	−52.30	−91.09, −13.51	0.012
vWF	34	−0.01	−0.06, 0.04	0.612	−0.01	−0.07, 0.05	0.703	−0.00	−0.06, 0.05	0.940	−0.00	−0.05, 0.05	0.873	0.00	−0.07, 0.07	0.975
% Predicted spirometry																
FEV_1	40	−0.52	−1.54, 0.50	0.293	−0.99	−1.98, −0.00	0.050	−1.60	−2.68, −0.51	0.006	−0.85	−1.76, 0.06	0.064	1.34	−0.05, 2.73	0.058
FVC	39	0.14	−0.74, 1.02	0.746	0.24	−0.71, 1.19	0.604	0.23	−0.92, 1.38	0.679	0.03	−0.84, 0.89	0.952	0.28	−1.09, 1.66	0.667
MMEF	39	0.27	−2.72, 3.25	0.851	−0.25	−3.47, 2.97	0.871	−1.41	−5.25, 2.42	0.444	1.03	−1.84, 3.89	0.457	0.48	−3.97, 4.92	0.822
PEFR	42	0.49	−3.33, 4.31	0.791	0.61	−3.39, 4.61	0.752	0.03	−5.09, 5.16	0.989	−1.62	−5.52, 2.29	0.396	2.75	−2.64, 8.13	0.298
Exhaled nitric oxide																
$\log(FeNO_{50,pred})$	41	−0.02	−0.06, 0.02	0.299	−0.02	−0.06, 0.02	0.377	0.00	−0.05, 0.05	0.974	0.00	−0.04, 0.04	0.945	−0.02	−0.07, 0.03	0.483
C_ANO	41	−0.07	−0.14, 0.01	0.082	−0.07	−0.15, 0.00	0.062	−0.05	−0.15, 0.05	0.336	−0.02	−0.10, 0.07	0.684	−0.05	−0.16, 0.06	0.357
$\log(C_{AW}NO)$	41	−0.07	−0.13, −0.00	0.044	−0.06	−0.13, 0.01	0.103	0.01	−0.08, 0.10	0.775	0.01	−0.06, 0.08	0.868	−0.06	−0.15, 0.02	0.144
$\log(D_{AW}NO)$	41	0.09	−0.02, 0.19	0.090	0.06	−0.05, 0.18	0.250	−0.05	−0.19, 0.08	0.418	−0.02	−0.12, 0.08	0.702	0.09	−0.04, 0.21	0.175

Pollutants

Outcome	N	PM_1			$PM_{2.5}$			PM_4			PM_{10}		
		Est	95% CI	*p*-Value	Est	95% CI	*p*-Value	Est	95% CI	*p*-Value	Est	95% CI	*p*-Value
Cytokines													
IL-6	36	−0.14	−0.29, 0.02	0.075	−0.19	−0.35, −0.04	0.015	−0.22	−0.37, −0.06	0.008	−0.31	−0.53, −0.08	0.010
Fibrinogen	35	−2.94	−11.71, 5.84	0.485	−4.45	−13.74, 4.84	0.322	−4.58	−14.21, 5.05	0.325	−9.54	−23.64, 4.55	0.169
sTNFrII	36	14.57	−19.19, 48.33	0.372	23.89	−11.45, 59.23	0.170	26.67	−9.73, 63.08	0.139	25.22	−31.18, 81.63	0.356
vWF	34	−0.00	−0.04, 0.04	0.956	−0.00	−0.05, 0.04	0.876	−0.01	−0.06, 0.04	0.766	−0.02	−0.10, 0.05	0.504
% Predicted spirometry													
FEV_1	40	−1.28	−2.04, −0.51	0.003	−1.45	−2.26, −0.64	0.002	−1.51	−2.35, −0.67	0.002	−2.02	−3.43, −0.61	0.008
FVC	39	0.50	−0.41, 1.40	0.260	0.43	−0.54, 1.40	0.358	0.42	−0.58, 1.43	0.386	0.46	−1.06, 1.99	0.527
MMEF	39	−2.90	−5.38, −0.41	0.025	−2.98	−5.76, −0.21	0.037	−3.08	−5.98, −0.19	0.038	−5.56	−9.83, −1.29	0.014
PEFR	42	2.49	−1.10, 6.08	0.163	2.22	−1.82, 6.27	0.263	2.17	−2.07, 6.42	0.296	3.30	−3.08, 9.68	0.292
Exhaled nitric oxide													
$\log(FeNO_{50,pred})$	41	0.01	−0.03, 0.04	0.723	−0.00	−0.04, 0.04	0.910	−0.01	−0.05, 0.04	0.764	−0.02	−0.08, 0.04	0.481
C_ANO	41	−0.02	−0.10, 0.05	0.497	−0.05	−0.13, 0.03	0.229	−0.06	−0.14, 0.03	0.173	−0.10	−0.22, 0.02	0.107
$\log(C_{AW}NO)$	41	0.00	−0.06, 0.07	0.913	0.01	−0.06, 0.08	0.767	0.01	−0.07, 0.08	0.799	0.02	−0.10, 0.13	0.755
$\log(D_{AW}NO)$	41	−0.03	−0.13, 0.07	0.541	−0.06	−0.17, 0.05	0.289	−0.06	−0.18, 0.05	0.282	−0.12	−0.29, 0.05	0.150

Source factors

Outcome	N	PM Mass			Traffic			Airport UFPs			Secondary photochemistry		
		Est	95% CI	*p*-Value	Est	95% CI	*p*-Value	Est	95% CI	*p*-Value	Est	95% CI	*p*-Value
Cytokines													
IL-6	36	−0.15	−0.31, 0.01	0.071	−0.06	−0.24, 0.11	0.457	0.21	0.08, 0.34	0.003	−0.20	−0.39, −0.01	0.044
Fibrinogen	35	−3.28	−12.52, 5.96	0.459	−2.60	−11.95, 6.74	0.560	1.74	−7.73, 11.21	0.699	−5.28	−16.36, 5.81	0.325

(*continued on next page*)

Table 5 (*continued*)

Source factors												
Outcome	N	PM Mass			Traffic			Airport UFPs			Secondary photochemistry		
		Est	95% CI	*p*-Value	Est	95% CI	*p*-Value	Est	95% CI	*p*-Value	Est	95% CI	*p*-Value
*s*TNFrII	36	13.77	−22.13, 49.68	0.426	36.47	6.03, 66.91	0.022	−5.21	−40.30, 29.89	0.756	27.83	−14.21, 69.87	0.179
vWF	34	−0.00	−0.05, 0.04	0.888	−0.00	−0.05, 0.05	0.933	−0.01	−0.05, 0.04	0.768	−0.01	−0.06, 0.05	0.777
% Predicted spirometry													
FEV_1	40	−1.31	−2.14, −0.49	0.004	−1.52	−2.28, −0.77	0.001	0.37	−0.62, 1.36	0.438	−1.55	−2.55, −0.54	0.005
FVC	39	0.52	−0.44, 1.48	0.270	0.25	−0.68, 1.19	0.574	−0.04	−0.91, 0.83	0.920	0.45	−0.68, 1.58	0.413
MMEF	39	−3.12	−5.75, −0.48	0.024	−1.48	−4.50, 1.53	0.311	1.49	−1.18, 4.17	0.252	−2.95	−6.43, 0.52	0.090
PEFR	42	2.70	−1.08, 6.47	0.151	0.39	−3.77, 4.56	0.845	−0.19	−4.08, 3.70	0.920	2.36	−2.26, 6.97	0.298
Exhaled nitric oxide													
$\log(FeNO_{50,pred})$	41	0.01	−0.03, 0.04	0.772	−0.00	−0.05, 0.04	0.873	−0.01	−0.05, 0.02	0.514	−0.01	−0.06, 0.03	0.568
C_ANO	41	−0.03	−0.11, 0.05	0.446	−0.05	−0.13, 0.04	0.244	−0.03	−0.10, 0.05	0.454	−0.08	−0.16, 0.01	0.073
$\log(C_{AW}NO)$	41	0.00	−0.07, 0.07	0.934	−0.00	−0.08, 0.07	0.947	−0.05	−0.11, 0.01	0.090	−0.01	−0.09, 0.08	0.884
$\log(D_{AW}NO)$	41	−0.03	−0.14, 0.07	0.518	−0.03	−0.14, 0.09	0.615	0.09	−0.00, 0.18	0.062	−0.05	−0.18, 0.08	0.464

Exposures: PN = Ultrafine Particle Number; LDSA = Lung-deposited surface area; PM_1, $PM_{2.5}$, PM_4, PM_{10} = Particle Mass in the 1, 2.5, 4 and 10 μm size fraction; BC = Black Carbon; PB-PAH = Particle-bound Polyaromatic Hydrocarbons; O_3 = Ozone.
Outcomes: Cytokines: IL6 = High-sensitivity Interleukin-6; sTNFrII = Soluble TNF receptor II; vWF = Von Willebrand Factor. Exhaled Nitric Oxide: FeNO50 = Predicted exhaled nitric oxide at 50 ml/s flow rate; C_ANO = Distal Alveolar Nitric Oxide; $C_{aw}NO$ = Airway Wall Nitric Oxide; $D_{aw}NO$ = Diffusivity. Lung Function (% predicted): FEV_1 = Forced Expiratory Volume in 1 s; FVC = Forced Vital Capacity; MMEF = Maximum Mid-expiratory Flow; PEFR = Peak Expiratory Flow Rate.
All reported effect estimates are scaled to one standard deviation change in the exposure of interest.

4. Discussion

We conducted a crossover panel study with a quasi-experimental design modeled after the McCreanor et al. (2007) study to investigate the effects of real-life exposure to airport-related UFPs on acute respiratory and systemic outcomes in 22 adults with asthma. Air pollution measurements and modeled source factor contributions reflected expected patterns at the two sites, and across both seasons of the study. We found significant increases in markers of systemic inflammation associated with 'Airport UFPs' (IL-6) and 'Traffic' (sTNFrII) exposure and a significant decrease in FEV_1 associated with measured PM and BC and modeled 'Traffic' exposure. The robust IL-6 effects we found with the 'Airport UFPs' source, which would have been masked by considering PN alone, suggest that some characteristic of the airport-related air pollution mixture as a whole might be more important for IL-6 response than particle number concentration. This could be the smaller particle size and alveolar deposition potential of airport-related UFPs (compared to overall PN which comingles airport and traffic contributions) or other gaseous, volatile or non-volatile components of the mixture that we did not measure or account for. To our knowledge, this is the first study to document acute systemic inflammation following airport-related UFPs exposure.

Most previous studies have investigated total or traffic-related personal UFP exposures. Buonanno et al. (2013) conducted personal monitoring for two days and found daily UFP alveolar-deposited surface area dose to be associated with increased exhaled nitric oxide and decreased FEV_1 ($-0.0025 \pm 0.0012\%$ per 100 mm^2 alveolar deposited surface area dose) in children with asthma and children with house dust mite allergies but no asthma. However, these children's daily UFP dose was dominated by indoor microenvironments (15% indoor home, 19% sleeping and 18% school) with a likely substantially different composition due to indoor UFP sources (Deffner et al., 2016; Gu et al., 2015; Vu et al., 2017; Wallace, 2006; Weichenthal et al., 2007) as compared to our study.

Steenhof et al. (2013) exposed 31 healthy volunteers to air pollution for 5 h while exercising at 3 of 5 sites in the Netherlands (2 traffic, 1 underground train station, 1 farm and 1 urban background site) and found NO_2 effects on proinflammatory cytokines measured in nasal lavage but no PN effects, while Janssen et al. (2015) found significant associations between measures of oxidative potential from 3 a-cellular assays with increased eNO and IL-6 in nasal lavage 2 h post exposure at all four outdoor sites (not including the underground metal-rich site). While not directly comparable to our study, these findings support the role of oxidative stress in acute inflammatory response following urban air pollution exposures and highlight the importance of considering composition.

In a panel study of 29 elderly subjects with coronary artery disease, Delfino et al. (2008) found a 7337 particles·cm^{-3}increase in outdoor PN was significantly associated with 0.50 pg/ml increase in IL-6 and 153.24 pg/ml increase in sTNFrII. PN and $PM_{0.25}$ (PM mass in the quasi-ultrafine size fraction, < 0.25 μm) were also more strongly associated with IL-6 and sTNFrII than $PM_{0.25–2.5}$ mass (Delfino et al., 2009). A 0.56 ng/m^3 increase in outdoor total PAHs was associated with 135 (45–225) pg/ml increase in sTNFrII and 0.27 (0.10–0.44) pg/ml increase in IL-6 (Delfino et al., 2010). However, PN in this study was mainly traffic-related (0.5 correlation with elemental carbon) and more closely resembled our 'Traffic' source with loadings of PN, BC and PB-PAHs. When taking particle composition into account, Delfino et al. (2010) found that $PM_{0.25}$ associations with IL-6 and sTNFrII were completely confounded by PAHs. The high correlation (0.85) between BC and PB-PAHs in our study meant that we could not include them in the same model; however, the 'Traffic' source captured their combined effect on sTNFrII. In general, higher effects were seen in the Delfino et al. studies for IL-6 and sTNFrII compared to our study, and this could be due to the differences in the composition and oxidative potential of the exposure mixtures (Delfino et al., 2011), or differences in

Table 6
Multi-pollutant model associations of measured concentrations and modeled source factor contributions with cytokines, exhaled nitric oxide and spirometry outcomes.

Pollutants

Outcome	N	PN			$PM_{2.5}$			BC			O_3		
		Est	95% CI	*p*-Value	Est	95% CI	*p*-Value	Est	95% CI	*p*-Value	Est	95% CI	*p*-Value
Cytokines													
IL-6	36	0.13	−0.02, 0.27	0.087	−0.28	−0.52, −0.05	0.023	0.13	−0.23, 0.50	0.438	0.05	−0.18, 0.28	0.659
Fibrinogen	35	−2.18	−15.17, 10.81	0.719	−9.56	−28.69, 9.56	0.294	10.07	−17.98, 38.13	0.446	7.31	−9.83, 24.44	0.368
sTNFrII	36	−3.11	−38.21, 31.99	0.850	−9.14	−69.37, 51.08	0.746	44.07	−48.54, 136.69	0.320	−33.28	−84.40, 17.83	0.181
vWF	34	−0.02	−0.10, 0.05	0.529	−0.02	−0.13, 0.09	0.659	0.03	−0.13, 0.20	0.646	0.02	−0.10, 0.14	0.702
% Predicted spirometry													
FEV_1	40	−0.75	−1.55, 0.05	0.065	−1.92	−3.13, −0.70	0.005	1.12	−0.71, 2.94	0.209	1.51	0.27, 2.75	0.021
FVC	39	0.24	−0.94, 1.43	0.661	0.75	−1.21, 2.72	0.418	−0.40	−3.25, 2.46	0.767	0.38	−1.56, 2.31	0.679
MMEF	39	−0.87	−4.19, 2.46	0.581	−5.31	−10.37, −0.25	0.041	4.25	−3.27, 11.77	0.242	1.42	−3.86, 6.71	0.569
PEFR	42	1.32	−3.92, 6.57	0.599	5.48	−2.14, 13.10	0.146	−5.47	−17.54, 6.61	0.350	1.00	−6.59, 8.60	0.782
Exhaled nitric oxide													
$\log(FeNO_{50,pred})$	41	−0.03	−0.08, 0.03	0.347	−0.02	−0.10, 0.06	0.617	0.03	−0.09, 0.15	0.596	0.00	−0.07, 0.07	0.995
C_ANO	41	−0.07	−0.18, 0.03	0.168	−0.08	−0.22, 0.07	0.295	0.05	−0.17, 0.28	0.610	−0.01	−0.15, 0.13	0.856
$\log(C_{AW}NO)$	41	−0.08	−0.16, 0.01	0.085	−0.02	−0.15, 0.10	0.697	0.06	−0.12, 0.24	0.501	−0.02	−0.13, 0.09	0.649
$\log(D_{AW}NO)$	41	0.10	−0.03, 0.23	0.129	−0.02	−0.21, 0.17	0.816	−0.06	−0.34, 0.23	0.678	0.05	−0.11, 0.21	0.506

Source factors

Outcome	N	PM Mass			Traffic			Airport UFPs			Secondary Photochemistry		
		Est	95% CI	*p*-Value	Est	95% CI	*p*-Value	Est	95% CI	*p*-Value	Est	95% CI	*p*-Value
Cytokines													
IL-6	36	0.05	−0.20, 0.31	0.652	0.09	−0.14, 0.31	0.423	0.18	0.04, 0.32	0.017	−0.29	−0.64, 0.07	0.102
Fibrinogen	35	1.24	−20.42, 22.90	0.902	2.63	−17.06, 22.31	0.775	0.26	−12.07, 12.58	0.964	−9.09	−38.13, 19.96	0.505
sTNFrII	36	−33.72	−97.38, 29.93	0.271	64.38	6.30, 122.46	0.033	−16.80	−51.64, 18.05	0.314	−6.45	−95.94, 83.04	0.878
vWF	34	0.00	−0.11, 0.11	0.981	0.01	−0.10, 0.12	0.785	−0.01	−0.07, 0.05	0.707	−0.03	−0.17, 0.12	0.709
% Predicted spirometry													
FEV_1	40	−0.63	−2.04, 0.78	0.353	−1.35	−2.80, 0.10	0.066	0.14	−0.76, 1.03	0.746	0.37	−1.58, 2.32	0.686
FVC	39	0.83	−1.13, 2.79	0.376	−0.46	−2.48, 1.55	0.626	0.33	−0.87, 1.52	0.564	0.27	−2.30, 2.84	0.821
MMEF	39	−3.48	−8.81, 1.84	0.180	1.80	−3.70, 7.31	0.489	−0.42	−3.89, 3.05	0.795	−1.66	−8.95, 5.62	0.628
PEFR	42	5.00	−1.87, 11.87	0.142	−5.57	−12.95, 1.80	0.128	2.02	−2.36, 6.41	0.341	3.32	−5.70, 12.34	0.445
Exhaled nitric oxide													
$\log(FeNO_{50,pred})$	41	0.02	−0.05, 0.10	0.539	0.01	−0.07, 0.10	0.756	−0.01	−0.06, 0.04	0.686	−0.05	−0.14, 0.04	0.298
C_ANO	41	0.01	−0.13, 0.15	0.878	0.04	−0.11, 0.19	0.595	−0.04	−0.13, 0.05	0.315	−0.13	−0.31, 0.04	0.120
$\log(C_{AW}NO)$	41	−0.04	−0.17, 0.09	0.494	0.04	−0.10, 0.17	0.546	−0.07	−0.15, 0.01	0.075	−0.02	−0.18, 0.13	0.758
$\log(D_{AW}NO)$	41	0.08	−0.13, 0.28	0.440	−0.05	−0.25, 0.15	0.580	0.11	−0.01, 0.23	0.077	−0.03	−0.28, 0.21	0.768

Exposures: PN = Ultrafine Particle Number; LDSA = Lung-deposited surface area; $PM_{2.5}$ = Particle Mass in the 2.5 μm size fraction; BC = Black Carbon; O_3 = Ozone.
Outcomes: Cytokines: IL6 = High-sensitivity Interleukin-6; sTNFrII = Soluble TNF receptor II; vWF = Von Willebrand Factor. Exhaled Nitric Oxide: FeNO50 = Predicted exhaled nitric oxide at 50 ml/s flow rate; C_ANO = Distal Alveolar Nitric Oxide; $C_{aw}NO$ = Airway Wall Nitric Oxide; $D_{aw}NO$ = Diffusivity. Lung Function (% predicted): FEV_1 = Forced Expiratory Volume in 1 s; FVC = Forced Vital Capacity; MMEF = Maximum Mid-expiratory Flow; PEFR = Peak Expiratory Flow Rate.
All reported effect estimates are scaled to one standard deviation change in the exposure of interest.

susceptibility of asthmatics compared to elderly participants with a history of coronary artery disease.

In the McCreanor et al. (2007) study, walking for 2 h in a diesel vehicular traffic zone with elevated $PM_{2.5}$, UFP, EC and NO_2 levels on Oxford Street, London, resulted in up to 6.1% and 5.4% decrease in FEV_1 and FVC compared to baseline, respectively, in asthmatics. Similarly, we found a 1.6% and 1.52% drop in % predicted FEV_1 2 h post BC and 'Traffic' exposure, respectively. In addition, we found that measured $PM_{2.5}$ was more strongly associated with reduced FEV_1 and MMEF than the modeled 'PM Mass' source, and that the PM_{10} size fraction had the largest effect on these lung function outcomes, suggesting that the actual PM mass or amount inhaled plays a role in worsening lung function, potentially related to increased burden on the lungs to clear particles from the airways.

$FeNO_{50}$ and airway NO source parameters were not associated with PN in our study, although associations have been previously reported in the literature (Buonanno et al., 2013; Strak et al., 2012). We also did not find any fibrinogen or vWF associations as previously reported in patients with chronic obstructive pulmonary disease (Hildebrandt et al., 2009).

Strengths of our study include: a randomized cross-over within-person, semi-experimental design; a susceptible study population (adults with asthma); participants who performed moderate-light activity to increase ventilation rates; randomized assignments to control and exposure scenarios with a 1+ week washout period in-between; exposures to real-life airport emissions; and the high exposure contrasts achieved at the two exposure locations. Using multi-pollutant measurements and source apportionment modeling, we distinguished the contribution of aviation activities at LAX from traffic, another major source of UFPs in this urban area. In addition, the use of personal monitoring accurately captured exposures in the breathing zone, while the DiscMini diffusion charger provided more detailed particle size and lung deposited surface area. Limitations of our study include a short follow up time, with only one health assessment ~ 2 h immediately after the walking exposure period, and the limited sample size in this pilot study that reduced statistical power. We were also unable to adjust for the variable inhalation rates across subjects due to varying levels of fitness, age, etc. but ensured an almost identical walking pace on all study days.

One of the biggest sources of uncertainty in estimating acute and chronic health effects of UFPs in epidemiological studies lies in the exposure assessment as noted by a European expert panel (Hoek et al., 2010). Specifically, for future airport-related UFP health investigations, it is important to consider the entire source to receptor pathway to accurately assess exposures and estimate health effects, starting from emissions, composition, fate and transport, exposures and confounding factors in the population of interest.

At low power conditions (thrust < 30%), commercial aircraft gas turbine engine emissions are dominated by organics –a variety of unburned hydrocarbons (ethylene, formaldehyde, acetaldehyde, and benzene) and lubrication oils. Whereas, higher power conditions are dominated (~80%) by soot or elemental carbon particles referred to as the non-volatile PM fraction (nvPM, the regulated fraction), which directly correlates with the fuel sulfur content (Onasch et al., 2009). As the plume cools downstream of the exhaust, volatile PM forms by two main processes: nucleation of exhaust gases such as SO_x creating new particles (< 20 nm, high PN and low mass) or condensation of gases onto existing soot particles (see Whitefield et al. (2011, 2008) for a detailed overview). Nucleation typically outnumbers condensation by a factor of 10 to 100 and is also dependent on fuel sulfur content (Lobo et al., 2007; Timko et al., 2010; Timko et al., 2013; Wong et al., 2015). Secondary organic aerosol formation in the aging plume likely exceeds primary organic aerosol emissions (Herndon et al., 2008; Presto et al., 2011). This is why measurements taken at the point of exit from the engine typically underestimate particle mass downwind by a factor of 5 to 10 (Timko et al., 2013).

As for composition, emitted nucleation mode particles are rich in carbon, oxygen, sulfur and chlorine (Mazaheri et al., 2013), and the oxidative reactivity of emitted soot particles is inversely proportional to thrust (Liati et al., 2014). Lubrication oil and incomplete combustion products are the primary sources of organics in emitted particles (Timko et al., 2010). Cross et al. (2013) resolved aliphatic, aromatic and oxygenated organics in aircraft emissions, mainly from unburned fuel at idling and from pyrolysis products at higher power. Timko et al. (2014) identified two lubrication oil factors, two aliphatic factors - one related to soot emissions and another to mixing with ambient organic aerosol – and a fifth factor related to benzene emissions at low thrust using the Positive Matrix Factorization (PMF) model.

Several modeling approaches have been used to predict the fine spatial and temporal variability in PN and separate the contribution of aircraft flight activity from other outdoor important UFP sources - namely traffic, fuel combustion, and secondary formation - ranging from statistical regression approaches (Diez et al., 2012; Hsu et al., 2012) to source-oriented and receptor-oriented source apportionment models. Source-oriented models include simple dispersion models such as a AERMOD that might perform well near the source but do not handle the complicated UFP particle dynamics and chemical transformations that are crucial determinants of the volatile PM fraction (Levy et al., 2015). More sophisticated source-oriented models include chemical transport models such as the Community Multiscale Air Quality (CMAQ) model that generally have lower spatial resolution but account for all sources and emissions in an urban area and fully model fate and transport with proper treatment of chemistry and particle dynamics and typically larger spatial domains that can capture communities further downwind (Arunachalam et al., 2011; Kukkonen et al., 2016; Levy et al., 2008; Levy et al., 2015; Levy et al., 2012). Receptor-oriented source apportionment models such as PMF or PCA used in our study have proven valuable for determining source impacts at affected communities and disentangling the airport signal from other potentially correlated UFP sources in the air pollution mixture (Masiol et al., 2016).

For all modeling efforts, detailed meteorological data and multiple pollutant measurements, including gases, semi-volatiles and particulate matter characteristics (composition, size distribution, particle number concentration, etc.) are recommended to characterize the mixture and obtain the best performance, especially in receptor models. While particle size and PN ratios relative to BC have been used to separate aircraft from traffic signals (Riley et al., 2016), an inert and unique chemical tracer of aircraft emissions would be ideal to facilitate source separation and minimize factor smearing in receptor models - possibly from the jet fuel formulation, lubrication oil additives or other compounds uniquely emitted by aircraft engines. The property of non-reactivity or known chemical reactivity where the species is conserved would facilitate the separation of aircraft impacts in fresh emissions as well as in more aged plumes downwind of airports.

Outdoor exposure estimates should be combined with information on individuals' time-activity patterns and UFP infiltration efficiency indoors to disentangle indoor- from outdoor-generated UFPs and isolate aviation/airport contributions to total personal UFP exposure. Cooking, smoking, burning wood, candles or incense, and cleaning are some of the indoor UFP sources (Habre et al., 2014; Vu et al., 2017; Wallace, 2006; Wallace et al., 2004). UFPs are generally less efficient at penetrating indoors compared to $PM_{2.5}$, with infiltration factors (F_{inf}) ranging from around 0 (particles < 10 nm) to 0.3 (particles between 80 and 100 nm) with windows closed and from 0 to 0.6 with one window open in a test house (Rim et al., 2010). Kearney et al. (2014) found large variability in UFP F_{inf} both within and between homes in Edmonton, with the majority of indoor UFPs being of indoor origin (contrary to indoor $PM_{2.5}$). Confounding from co-occurring exposures such as noise or socioeconomic factors related to health disparities should also be adjusted for in epidemiological studies of aviation-related UFP exposures. Finally, recent advances in miniaturization of personal UFP monitors combined with detailed time-activity and

geolocation tracking to capture individuals' behaviors and time spent in various microenvironments can prove crucial in estimating the contribution of aviation-related sources to total personal UFP exposure, especially in heavily exposed occupational subgroups such as baggage handlers (Moller et al., 2014; Moller et al., 2017).

In conclusion, and up to our knowledge, our study is the first to demonstrate increased acute systemic inflammation following exposure to airport-related UFPs. These effects were distinct from traffic-related exposures. Further research is needed to replicate these findings in different susceptible populations and at longer time lags to determine downstream health effects, especially in communities heavily impacted by multiple environmental exposures. This study also emphasizes the importance of multi-pollutant measurements and modeling techniques to disentangle sources of UFPs contributing to the complex urban air pollution mixture and to evaluate population health risks.

Acknowledgements

This study was funded by the Southern California Environmental Health Sciences Center (National Institute of Environmental Health Sciences, P30ES007048) pilot program, NIEHS grants 1R01ES023262, 1K22ES022987, 1R01ES027860, and the Hastings Foundation. The authors gratefully acknowledge Ashley Erickson, Michael Chon, Nicholas Gedeon, Suresh Ratnam, Steve Howland, Jane Cabison and Milena Amadeus for their assistance in conducting the study and all the participants for their time and effort. The authors also gratefully thank Dr. Robert Giannelli, Mr. Chad Bailey, Mr. John Kinsey, and Mr. Bryan Manning of the United States Environmental Protection Agency Office of Transportation and Air Quality for sharing their tremendous knowledge and expertise on composition, characteristics and testing protocols of commercial aircraft emissions.

Competing financial interests

The authors declare no competing financial interests.

Appendix A. Supplementary data

Supplementary data to this article can be found online at https://doi.org/10.1016/j.envint.2018.05.031.

References

ACI Europe, 2012. Ultrafine particles at airports: discussion and assessment of ultrafine particles (ufp) in aviation and at airports in 2012. In: Environmental Strategy Committee of Airports Council International ACI EUROPE.
Araujo, J.A., Nel, A.E., 2009. Particulate matter and atherosclerosis: role of particle size, composition and oxidative stress. Part. Fibre Toxicol. 6, 24.
Arunachalam, S., Wang, B.Y., Davis, N., Baek, B.H., Levy, J.I., 2011. Effect of chemistry-transport model scale and resolution on population exposure to pm2.5 from aircraft emissions during landing and takeoff. Atmos. Environ. 45, 3294–3300.
ATS/ERS, 2005. Ats/ers recommendations for standardized procedures for the online and offline measurement of exhaled lower respiratory nitric oxide and nasal nitric oxide, 2005. Am. J. Respir. Crit. Care Med. 171, 912–930.
Ayres, J.G., Borm, P., Cassee, F.R., Castranova, V., Donaldson, K., Ghio, A., et al., 2008. Evaluating the toxicity of airborne particulate matter and nanoparticles by measuring oxidative stress potential - a workshop report and consensus statement. Inhal. Toxicol. 20, 75–99.
Brauer, M., Hoek, G., Van Vliet, P., Meliefste, K., Fischer, P.H., Wijga, A., et al., 2002. Air pollution from traffic and the development of respiratory infections and asthmatic and allergic symptoms in children. Am. J. Respir. Crit. Care Med. 166, 1092–1098.
Buonanno, G., Marks, G.B., Morawska, L., 2013. Health effects of daily airborne particle dose in children: direct association between personal dose and respiratory health effects. Environ. Pollut. 180, 246–250.
Cho, A.K., Sioutas, C., Miguel, A.H., Kumagai, Y., Schmitz, D.A., Singh, M., et al., 2005. Redox activity of airborne particulate matter at different sites in the los Angeles basin. Environ. Res. 99, 40–47.
Choi, W., Hu, S.S., He, M.L., Kozawa, K., Mara, S., Winer, A.M., et al., 2013. Neighborhood-scale air quality impacts of emissions from motor vehicles and aircraft. Atmos. Environ. 80, 310–321.
Cross, E.S., Hunter, J.F., Carrasquillo, A.J., Franklin, J.P., Herndon, S.C., Jayne, J.T., et al., 2013. Online measurements of the emissions of intermediate-volatility and semi-volatile organic compounds from aircraft. Atmos. Chem. Phys. 13, 7845–7858.
Deffner, V., Kuechenhoff, H., Maier, V., Pitz, M., Cyrys, J., Breitner, S., et al., 2016. Personal exposure to ultrafine particles: two-level statistical modeling of background exposure and time-activity patterns during three seasons. J. Expo. Sci. Environ. Epidemiol. 26, 17–25.
Delfino, R.J., Sioutas, C., Malik, S., 2005. Potential role of ultrafine particles in associations between airborne particle mass and cardiovascular health. Environ. Health Perspect. 113, 934–946.
Delfino, R.J., Staimer, N., Tjoa, T., Polidori, A., Arhami, M., Gillen, D.L., et al., 2008. Circulating biomarkers of inflammation, antioxidant activity, and platelet activation are associated with primary combustion aerosols in subjects with coronary artery disease. Environ. Health Perspect. 116, 898–906.
Delfino, R.J., Staimer, N., Tjoa, T., Gillen, D.L., Polidori, A., Arhami, M., et al., 2009. Air pollution exposures and circulating biomarkers of effect in a susceptible population: clues to potential causal component mixtures and mechanisms. Environ. Health Perspect. 117, 1232–1238.
Delfino, R.J., Staimer, N., Tjoa, T., Arhami, M., Polidori, A., Gillen, D.L., et al., 2010. Association of biomarkers of systemic inflammation with organic components and source tracers in quasi-ultrafine particles. Environ. Health Perspect. 118, 756–762.
Delfino, R.J., Staimer, N., Vaziri, N.D., 2011. Air pollution and circulating biomarkers of oxidative stress. Air Qual. Atmos. Health 4, 37–52.
Diez, D.M., Dominici, F., Zarubiak, D., Levy, J.I., 2012. Statistical approaches for identifying air pollutant mixtures associated with aircraft departures at Los Angeles international airport. Environ. Sci. Technol. 46, 8229–8235.
Eckel, S.P., Salam, M.T., 2013. Single high flow exhaled nitric oxide is an imperfect proxy for distal nitric oxide. Occup. Environ. Med. 70, 519–520.
Eckel, S.P., Linn, W.S., Berhane, K., Rappaport, E.B., Salam, M.T., Zhang, Y., et al., 2014. Estimation of parameters in the two-compartment model for exhaled nitric oxide. PLoS One 9, e85471.
Eckel, S.P., Zhang, Z., Habre, R., Rappaport, E.B., Linn, W.S., Berhane, K., et al., 2016. Traffic-related air pollution and alveolar nitric oxide in southern California children. Eur. Respir. J. 47, 1348–1356.
Elder, A., Gelein, R., Silva, V., Feikert, T., Opanashuk, L., Carter, J., et al., 2006. Translocation of inhaled ultrafine manganese oxide particles to the central nervous system. Environ. Health Perspect. 114, 1172–1178.
Gauderman, W.J., Avol, E., Lurmann, F., Kuenzli, N., Gilliland, F., Peters, J., et al., 2005. Childhood asthma and exposure to traffic and nitrogen dioxide. Epidemiology 16, 737–743.
Geiser, M., 2010. Update on macrophage clearance of inhaled micro- and nanoparticles. J. Aerosol Med. Pulm. Drug Deliv. 23, 207–217.
Gong, J., Zhu, T., Kipen, H., Wang, G., Hu, M., Guo, Q., et al., 2014. Comparisons of ultrafine and fine particles in their associations with biomarkers reflecting physiological pathways. Environ. Sci. Technol. 48, 5264–5273.
Gu, J.W., Kraus, U., Schneider, A., Hampel, R., Pitz, M., Breitner, S., et al., 2015. Personal day-time exposure to ultrafine particles in different micro environments. Int. J. Hyg. Environ. Health 218, 188–195.
Habre, R., Coull, B., Moshier, E., Godbold, J., Grunin, A., Nath, A., et al., 2014. Sources of indoor air pollution in New York city residences of asthmatic children. J. Expo. Sci. Environ. Epidemiol. 24, 269–278.
Heinzerling, A., Hsu, J., Yip, F., 2016. Respiratory health effects of ultrafine particles in children: a literature review. Water Air Soil Pollut. 227, 32.
Herndon, S.C., Jayne, J.T., Lobo, P., Onasch, T.B., Fleming, G., Hagen, D.E., et al., 2008. Commercial aircraft engine emissions characterization of in-use aircraft at Hartsfield-Jackson Atlanta international airport. Environ. Sci. Technol. 42, 1877–1883.
Hildebrandt, K., Ruckerl, R., Koenig, W., Schneider, A., Pitz, M., Heinrich, J., et al., 2009. Short-term effects of air pollution: a panel study of blood markers in patients with chronic pulmonary disease. Part. Fibre Toxicol. 6.
Hoek, G., Boogaard, H., Knol, A., de Hartog, J., Slottje, P., Ayres, J.G., et al., 2010. Concentration response functions for ultrafine particles and all-cause mortality and hospital admissions: results of a european expert panel elicitation. Environ. Sci. Technol. 44, 476–482.
Hofman, J., Staelens, J., Cordell, R., Stroobants, C., Zikova, N., Hama, S.M.L., et al., 2016. Ultrafine particles in four european urban environments: results from a new continuous long-term monitoring network. Atmos. Environ. 136, 68–81.
Hsu, H.H., Adamkiewicz, G., Houseman, E.A., Vallarino, J., Melly, S.J., Wayson, R.L., et al., 2012. The relationship between aviation activities and ultrafine particulate matter concentrations near a mid-sized airport. Atmos. Environ. 50, 328–337.
Hsu, H.H., Adamkiewicz, G., Houseman, E.A., Zarubiak, D., Spengler, J.D., Levy, J.I., 2013. Contributions of aircraft arrivals and departures to ultrafine particle counts near Los Angeles international airport. Sci. Total Environ. 444, 347–355.
Hsu, H.H., Adamkiewicz, G., Houseman, E.A., Spengler, J.D., Levy, J.I., 2014. Using mobile monitoring to characterize roadway and aircraft contributions to ultrafine particle concentrations near a mid-sized airport. Atmos. Environ. 89, 688–695.
Hudda, N., Fruin, S.A., 2016. International airport impacts to air quality: size and related properties of large increases in ultrafine particle number concentrations. Environ. Sci. Technol. 50, 3362–3370.
Hudda, N., Gould, T., Hartin, K., Larson, T.V., Fruin, S.A., 2014. Emissions from an international airport increase particle number concentrations 4-fold at 10 km downwind. Environ. Sci. Technol. 48, 6628–6635.
Hudda, N., Simon, M.C., Zamore, W., Brugge, D., Durant, J.L., 2016. Aviation emissions impact ambient ultrafine particle concentrations in the greater Boston area. Environ. Sci. Technol. 50, 8514–8521.
Janssen, N.A., Strak, M., Yang, A., Hellack, B., Kelly, F.J., Kuhlbusch, T.A., et al., 2015. Associations between three specific a-cellular measures of the oxidative potential of particulate matter and markers of acute airway and nasal inflammation in healthy volunteers. Occup. Environ. Med. 72, 49–56.

Kearney, J., Wallace, L., MacNeill, M., Héroux, M.-E., Kindzierski, W., Wheeler, A., 2014. Residential Infiltration of Fine and Ultrafine Particles in Edmonton. 94. pp. 793–805.
Keuken, M.P., Moerman, M., Zandveld, P., Henzing, J.S., Hoek, G., 2015. Total and size-resolved particle number and black carbon concentrations in urban areas near schiphol airport (the Netherlands). Atmos. Environ. 104, 132–142.
Knibbs, L.D., Cole-Hunter, T., Morawska, L., 2011. A review of commuter exposure to ultrafine particles and its health effects. Atmos. Environ. 45, 2611–2622.
Knudson, R.J., Lebowitz, M.D., Holberg, C.J., Burrows, B., 1983. Changes in the normal maximal expiratory flow-volume curve with growth and aging. Am. Rev. Respir. Dis. 127, 725–734.
Kukkonen, J., Karl, M., Keuken, M.P., van der Gon, H., Denby, B.R., Singh, V., et al., 2016. Modelling the dispersion of particle numbers in five european cities. Geosci. Model Dev. 9, 451–478.
Kunzli, N., Kaiser, R., Medina, S., Studnicka, M., Chanel, O., Filliger, P., et al., 2000. Public-health impact of outdoor and traffic-related air pollution: a European assessment. Lancet 356, 795–801.
Lai, S.K., Wang, Y.Y., Hanes, J., 2009. Mucus-penetrating nanoparticles for drug and gene delivery to mucosal tissues. Adv. Drug Deliv. Rev. 61, 158–171.
Lanzinger, S., Schneider, A., Breitner, S., Stafoggia, M., Erzen, I., Dostal, M., et al., 2016. Associations between ultrafine and fine particles and mortality in five central european cities - results from the ufireg study. Environ. Int. 88, 44–52.
Levy, J., Hsu, H.-H., Melly, S., 2008. High Priority Compounds Associated with Aircraft Emissions. Partner Project 11 Final Report on Subtask: Health Risk Prioritization of Aircraft Emissions Related Air Pollutants.
Levy, J.I., Woody, M., Baek, B.H., Shankar, U., Arunachalam, S., 2012. Current and future particulate-matter-related mortality risks in the United States from aviation emissions during landing and takeoff. Risk Anal. 32, 237–249.
Levy, J., Hsu, H.-H., Zhou, Y., Penn, S., Dodson, R., Diez, D., et al., 2015. Health impacts of aviation-related air pollutants. In: Partner Project 11 Final Report.
Li, N., Sioutas, C., Cho, A., Schmitz, D., Misra, C., Sempf, J., et al., 2003. Ultrafine particulate pollutants induce oxidative stress and mitochondrial damage. Environ. Health Perspect. 111, 455–460.
Liati, A., Brem, B.T., Durdina, L., Vogtli, M., Dasilva, Y.A.R., Eggenschwiler, P.D., et al., 2014. Electron microscopic study of soot particulate matter emissions from aircraft turbine engines. Environ. Sci. Technol. 48, 10975–10983.
Linn, W.S., Rappaport, E.B., Berhane, K.T., Bastain, T.M., Salam, M.T., Gilliland, F.D., 2009. Extended exhaled nitric oxide analysis in field surveys of schoolchildren: a pilot test. Pediatr. Pulmonol. 44, 1033–1042.
Lobo, P., Hagen, D.E., Whitefield, P.D., Alofs, D.J., 2007. Physical characterization of aerosol emissions from a commercial gas turbine engine. J. Propuls. Power 23, 919–929.
Masiol, M., Vu, T.V., Beddows, D.C.S., Harrison, R.M., 2016. Source apportionment of wide range particle size spectra and black carbon collected at the airport of Venice (Italy). Atmos. Environ. 139, 56–74.
Massachusetts Department of Public Health, 2014. Logan Airport Health Study. Massachusetts Department of Public Health.
Mazaheri, M., Bostrom, T.E., Johnson, G.R., Morawska, L., 2013. Composition and morphology of particle emissions from in-use aircraft during takeoff and landing. Environ. Sci. Technol. 47, 5235–5242.
McConnell, R., Berhane, K., Yao, L., Jerrett, M., Lurmann, F., Gilliland, F., et al., 2006. Traffic, susceptibility, and childhood asthma. Environ. Health Perspect. 114, 766–772.
McCreanor, J., Cullinan, P., Nieuwenhuijsen, M.J., Stewart-Evans, J., Malliarou, E., Jarup, L., et al., 2007. Respiratory effects of exposure to diesel traffic in persons with asthma. N. Engl. J. Med. 357, 2348–2358.
Metcalfe, C., 2010. The Analysis of Cross-over Trials with Baseline Measurements. 29. pp. 3211–3218.
Miller, M.R., Hankinson, J., Brusasco, V., Burgos, F., Casaburi, R., Coates, A., et al., 2005. Standardisation of spirometry. Eur. Respir. J. 26, 319–338.
Möller, W., Felten, K., Sommerer, K., Scheuch, G., Meyer, G., Meyer, P., et al., 2008. Deposition, retention, and translocation of ultrafine particles from the central airways and lung periphery. Am. J. Respir. Crit. Care Med. 177, 426–432.
Moller, K.L., Thygesen, L.C., Schipperijn, J., Loft, S., Bonde, J.P., Mikkelsen, S., et al., 2014. Occupational exposure to ultrafine particles among airport employees - combining personal monitoring and global positioning system. PLoS One 9.
Moller, K.L., Brauer, C., Mikkelsen, S., Loft, S., Simonsen, E.B., Koblauch, H., et al., 2017. Copenhagen airport cohort: air pollution, manual baggage handling and health. BMJ Open 7.
Nel, A., 2005. Atmosphere. Air pollution-related illness: effects of particles. Science 308, 804–806.
Nel, A.E., Diaz-Sanchez, D., Fau-Li, N., Li, N., 2001. The role of particulate pollutants in pulmonary inflammation and asthma: evidence for the involvement of organic chemicals and oxidative stress. Curr. Opin. Pulm. Med. 7, 20–26.
Nemmar, A., Hoylaerts, M.F., Hoet, P.H.M., Nemery, B., 2004. Possible mechanisms of the cardiovascular effects of inhaled particles: systemic translocation and prothrombotic effects. Toxicol. Lett. 149, 243–253.
Onasch, T.B., Jayne, J.T., Herndon, S., Worsnop, D.R., Miake-Lye, R.C., Mortimer, I.P., et al., 2009. Chemical properties of aircraft engine particulate exhaust emissions. J. Propuls. Power 25, 1121–1137.
Peters, A., Hampel, R., Cyrys, J., Breitner, S., Geruschkat, U., Kraus, U., et al., 2015. Elevated particle number concentrations induce immediate changes in heart rate variability: a panel study in individuals with impaired glucose metabolism or diabetes. Part. Fibre Toxicol. 12.
Presto, A.A., Nguyen, N.T., Ranjan, M., Reeder, A.J., Lipsky, E.M., Hennigan, C.J., et al., 2011. Fine particle and organic vapor emissions from staged tests of an in-use aircraft engine. Atmos. Environ. 45, 3603–3612.
Puckett, J.L., Taylor, R.W., Galant, S.P., George, S.C., 2010. Impact of analysis interval on the multiple exhalation flow technique to partition exhaled nitric oxide. Pediatr. Pulmonol. 45, 182–191.
Riley, E.A., Gould, T., Hartin, K., Fruin, S.A., Simpson, C.D., Yost, M.G., et al., 2016. Ultrafine particle size as a tracer for aircraft turbine emissions. Atmos. Environ. 139, 20–29.
Rim, D., Wallace, L., Persily, A., 2010. Infiltration of outdoor ultrafine particles into a test house. Environ. Sci. Technol. 44, 5908–5913.
Ruckerl, R., Ibald-Mulli, A., Koenig, W., Schneider, A., Woelke, G., Cyrys, J., et al., 2006. Air pollution and markers of inflammation and coagulation in patients with coronary heart disease. Am. J. Respir. Crit. Care Med. 173, 432–441.
Samet, J.M., Rappold, A., Graff, D., Cascio, W.E., Berntsen, J.H., Huang, Y.C., et al., 2009. Concentrated ambient ultrafine particle exposure induces cardiac changes in young healthy volunteers. Am. J. Respir. Crit. Care Med. 179, 1034–1042.
Schlenker, W., Walker, R., 2011. Airports, Air Pollution and Contemporaneous Health. (NBER Working Paper No 17684). National Bureau of Economic Research, Cambridge, MA.
Schuster, B.S., Suk, J.S., Woodworth, G.F., Hanes, J., 2013. Nanoparticle diffusion in respiratory mucus from humans without lung disease. Biomaterials 34, 3439–3446.
Shirmohammadi, F., Sowlat, M.H., Hasheminassab, S., Saffari, A., Ban-Weiss, G., Sioutas, C., 2017. Emission rates of particle number, mass and black carbon by the Los Angeles international airport (lax) and its impact on air quality in Los Angeles. Atmos. Environ. 151, 82–93.
Sinharay, R., Gong, J., Barratt, B., Ohman-Strickland, P., Ernst, S., Kelly, F.J., et al., 2018. Respiratory and cardiovascular responses to walking down a traffic-polluted road compared with walking in a traffic-free area in participants aged 60 years and older with chronic lung or heart disease and age-matched healthy controls: a randomised, crossover study. Lancet 391, 339–349.
Sioutas, C., Delfino, R.J., Singh, M., 2005. Exposure assessment for atmospheric ultrafine particles (ufps) and implications in epidemiologic research. Environ. Health Perspect. 113, 947–955.
Steenhof, M., Mudway, I.S., Gosens, I., Hoek, G., Godri, K.J., Kelly, F.J., et al., 2013. Acute nasal pro-inflammatory response to air pollution depends on characteristics other than particle mass concentration or oxidative potential: the raptes project. Occup. Environ. Med. 70, 341–348.
Stolzel, M., Breitner, S., Cyrys, J., Pitz, M., Wolke, G., Kreyling, W., et al., 2007. Daily Mortality and Particulate Matter in Different Size Classes in Erfurt, Germany. 17. pp. 458.
Strak, M., Janssen, N.A., Godri, K.J., Gosens, I., Mudway, I.S., Cassee, F.R., et al., 2012. Respiratory health effects of airborne particulate matter: the role of particle size, composition, and oxidative potential-the raptes project. Environ. Health Perspect. 120, 1183–1189.
Timko, M.T., Onasch, T.B., Northway, M.J., Jayne, J.T., Canagaratna, M.R., Herndon, S.C., et al., 2010. Gas turbine engine emissions-part ii: chemical properties of particulate matter. J. Eng. Gas Turbines Power 132.
Timko, M.T., Fortner, E., Franklin, J., Yu, Z., Wong, H.W., Onasch, T.B., et al., 2013. Atmospheric measurements of the physical evolution of aircraft exhaust plumes. Environ. Sci. Technol. 47, 3513–3520.
Timko, M.T., Albo, S.E., Onasch, T.B., Fortner, E.C., Yu, Z.H., Miake-Lye, R.C., et al., 2014. Composition and sources of the organic particle emissions from aircraft engines. Aerosol Sci. Technol. 48, 61–73.
Vitkina, T.I., Yankova, V.I., Gvozdenko, T.A., Kuznetsov, V.L., Krasnikov, D.V., Nazarenko, A.V., et al., 2016. The impact of multi-walled carbon nanotubes with different amount of metallic impurities on immunometabolic parameters in healthy volunteers. Food Chem. Toxicol. 87, 138–147.
Vu, T.V., Ondracek, J., Zdímal, V., Schwarz, J., Delgado-Saborit, J.M., Harrison, R.M., 2017. Physical properties and lung deposition of particles emitted from five major indoor sources. Air Qual. Atmos. Health 10, 1–14.
Wallace, L., 2006. Indoor sources of ultrafine and accumulation mode particles: size distributions, size-resolved concentrations, and source strengths. Aerosol Sci. Technol. 40, 348–360.
Wallace, L.A., Emmerich, S.j., Fau-Howard-Reed, C., Howard-Reed, C., 2004. Source Strengths of Ultrafine and Fine Particles due to Cooking with a Gas Stove. Environ. Sci. Technol. 38 (8), 2304–2311.
Weichenthal, S., Dufresne A Fau-Infante-Rivard, C., Infante-Rivard, C., 2007. Indoor ultrafine particles and childhood asthma: exploring a potential public health concern. Indoor Air 17, 81–91.
Westerdahl, D., Fruin, S.A., Fine, P.L., Sioutas, C., 2008. The Los Angeles international airport as a source of ultrafine particles and other pollutants to nearby communities. Atmos. Environ. 42, 3143–3155.
Whitefield, P.D., Lobo, P., Hagen, D., Timko, M., Miake-Lye, R., Taylor, C., et al., 2008. Summarizing and Interpreting Aircraft Gaseous and Particulate Emissions Data. National Academies Press, Washington, DC.
Whitefield, Hagen D., Lobo, P., Knighton, W., Bulzan, D., Tacina, K., et al., 2011. Alternative Aviation Fuel Experiment (Aafex). National Aeronautics and Space Administration, Hanover, MD.
Wichmann, H.E., Spix, C., Tuch, T., Wolke, G., Peters, A., Heinrich, J., et al., 2000. Epidemiological Evidence of the Effects of Ultrafine Particle Exposure. 5–86. pp. 87.
Wong, H.W., Jun, M., Peck, J., Waitz, I.A., Miake-Lye, R.C., 2015. Roles of organic emissions in the formation of near field aircraft-emitted volatile particulate matter: a kinetic microphysical modeling study. J. Eng. Gas Turbines Power 137.
Xu, Q., Boylan, N.J., Cai, S., Miao, B., Patel, H., Hanes, J., 2013. Scalable method to produce biodegradable nanoparticles that rapidly penetrate human mucus. J. Control. Release 170, 279–286.